AIAA JOURNAL
Vol. 33, No. 4, April 1995

Variational Principles for Ascent Shapes of Large Scientific Balloons

Frank Baginski* and Sita Ramamurti†
George Washington University, Washington, D.C. 20052

Current mathematical models of large scientific balloons assume an axisymmetric ascent shape, sharply contrasting what is observed in real balloons. We propose an approach to computing nonaxisymmetric shapes of balloons which is based on the inextensibility of certain balloon fibers and a set of rules that model how excess material must fold away. The energy of a balloon configuration is modeled as the sum of the gravitational potentials of the lifting gas and balloon fabric. We evolve an initial guess to a shape that minimizes this energy while satisfying certain material constraints. We refer to a shape determined in this fashion as an energy-minimizing (EM) shape. Using our approach to compute axisymmetric EM shapes, we find our results agree with those obtained by solving the standard Σ-shape model. For nonaxisymmetric shapes, we are able to compute shapes that possess features observed in actual balloons, including internally folded material, flat wing sections, and periodic lobe-like structures surrounding the gas bubble.

Nomenclature

$\mathcal{A}_{\text{float}}$	= balloon surface area at float altitude
$\mathcal{A}_i$	= area of $\mathcal{F}_i$
$\mathcal{C}_k$	= class of piecewise differentiable surfaces with D_k symmetry
D_k	= dihedral group, group of motions of the plane generated by rotations about the origin through an angle of $2\pi/k$ and reflections about some fixed axis
E	= sum of the gravitational potential energy of the lifting gas E_{gas} and the gravitational potential energy of the balloon film E_{film}
$e^c_{k,j}$	= length of kth segment of jth circumferential fiber
$e^m_{k,j}$	= length of kth segment of jth meridional fiber
$\mathcal{F}_i$	= facet in an approximation of $\mathcal{S}$
g	= acceleration due to gravity
ℓ	= length of a meridian, gore length
$N_{\mathcal{F}}$	= number of facets $\mathcal{F}_i$
N_v	= number of vertices in a fundamental section
n_c	= number of segments in a circumferential fiber
n_m	= number of segments in a meridional fiber
$\mathcal{P}_{\text{hook}}$	= hook plane, $\{(x, y, z) \in R^3 \mid y = 0\}$
$\mathcal{P}_{\text{wing}}$	= wing plane, $\{(x, y, z) \in R^3 \mid y = \tan(\pi/k)x\}$ for some positive integer k, corresponding to the dihedral group D_k
$(R(s), Z(s))$	= generating curve for the float shape
$(r(s), z(s))$	= generating curve for an axisymmetric shape
$\mathcal{S}$	= balloon surface
$\mathcal{S}_{\text{fund}}$	= fundamental section of an asymmetric ascent shape
$\mathcal{S}'_{\text{fund}}$	= reflection of $\mathcal{S}_{\text{fund}}$ in the $y = 0$ plane
s	= arc length measured along a meridian, gore
$\mathcal{V}$	= gas volume of balloon surface $\mathcal{S}$
$\mathcal{V}_{\text{float}}$	= gas volume at float altitude
$\mathcal{V}_i$	= volume of tetrahedron formed by joining vertices of $\mathcal{F}_i$ to a base point on z axis inside gas bubble
$\mathcal{W}$	= $\{(x, y, z) \in R^3 \mid 0 \le y \le \tan(\pi/k)x\}$
$z_{\max}$	= balloon height measured along the central axis from tail to apex
θ_0	= cone angle of axisymmetric shape, $\arctan[r'(0)/z'(0)]$
μ	= constant, proportional to $g \cdot \rho_{\text{film}}$
ρ	= constant for a fixed altitude, $g(\rho_{\text{gas}} - \rho_{\text{air}})$
ρ_{air}	= density of ambient air, mass per unit volume
ρ_{film}	= balloon film density, mass per unit area
ρ_{gas}	= density of the lifting gas, mass per unit volume

Received Dec 1, 1993; revision received May 20, 1994; accepted for publication May 23, 1994.

*Associate Professor, Department of Mathematics. Member AIAA.
†Graduate Student, Department of Mathematics.

I. Introduction

CURRENT design criteria for large scientific balloons are determined largely by conditions that the balloon will encounter at its float altitude.[1] Usually, the balloon shape is modeled by a system of nonlinear differential equations which was developed at the University of Minnesota.[2] Solutions of this system of equations are called Σ shapes. Smalley did extensive numerical calculations using this model (see, for example, Ref. 3). Boundary conditions for these equations are based on factors such as payload, balloon film weight, volume, and float altitude. Solutions at float and during ascent are assumed to be axisymmetric. In practice, the distribution of excess material below float is handled in an ad hoc fashion. For example, one could assume all excess material is contained within a rope section that hangs beneath the base of the balloon. See Fig. 1 for Σ shapes at float and below float.

Based on observations of actual balloons, it is clear that the typical shape of a balloon during ascent is not axisymmetric. To describe accurately the behavior of a real balloon, it is essential that the axisymmetric shape assumption be dropped and that the model reflect observed features. In particular, fold-like features need to be incorporated into the mathematical model.

There are two main points in our work that we wish to bring out in this paper. The first centers on modeling fold-like features of balloons. The second involves an approach to computing equilibrium shapes via a minimum energy principle. The behavior of a real balloon is complicated, and we must make certain simplifying assumptions. For our model, the surface of the balloon is defined by a set of vertices lying on a grid of inextensible circumferential and meridional fibers. These fibers are allowed to slide past one another. The intrinsic distance between two adjacent vertices on a fiber may change, but the total length of the fiber is preserved. The total surface area of the balloon at float is also preserved. However, this does not mean that the film is inextensible in the sense of a membrane. We ignore effects such as the stretching or wrinkling of the balloon fabric. The energy-minimizing EM shape is formed by the interaction of the lifting gas constrained by the faceted surface as defined by the set of vertices just described.

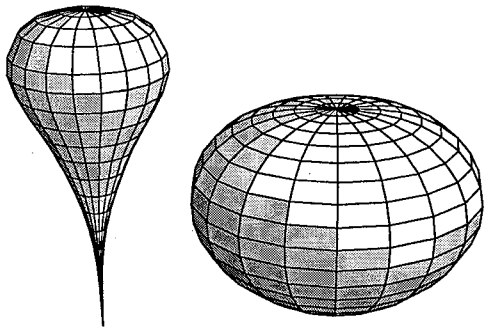

Fig. 1 Σ shapes: below float (left) and at float (right).

For the axisymmetric cases, we compute shapes that agree with those obtained by solving the Σ-shape equations with a shooting method, suggesting a variational principle for nonaxisymmetric shapes. One advantage of our variational approach is that fold-like features characterizing ascent shapes can be incorporated in a very natural way.

In Sec. II we describe our approach to modeling fold-like features in balloons. In some ways our problem for a balloon is analogous to the classical problem of determining the shape of an inextensible chain hanging between two fixed points. The equilibrium shape of the chain (a catenoid) can be computed by minimizing the gravitational potential energy of the chain subject to appropriate boundary conditions and fixed chain length. This motivates our variational principles for EM shapes. In Sec. III we present a variational formulation for computing EM shapes and derive discrete approximations to these constrained minimization problems. In Sec. IV we compute axisymmetric EM shapes and find good agreement with the solutions of the Σ-shape equations. In Sec. V we compute an example of an asymmetric EM shape with heptagonal symmetry and fold-like features.

II. Modeling Fold-Like Features

In Ref. 4, the author describes a method of constructing a nonaxisymmetric balloon shape, based on the inextensibility of balloon fibers, preservation of balloon surface area, and a set of rules that model how excess material must fold away. This report identified three types of fold-like features (see Fig. 2) which were observed in real balloons: 1) clefts—V-shaped indented formations running from top to bottom of the balloon, 2) wings—flat sections, starting near the base of the gas bubble and running to the bottom of the balloon, and 3) internal folds—flat sections, folded inward, directed toward the center axis of the balloon, running parallel to the load tapes, and contained inside the gas bubble.

The release of a large scientific balloon from the launch spool is very dynamic event. In this work, we are concerned with shapes which are observed before float altitude is reached but long enough after launch so that the balloon has had a chance to settle down. The ascent to float altitude is slow, usually taking on the order of several hours. A shape generated by our model should be viewed as a snapshot of a balloon taken at fixed altitude (or equivalently, fixed volume). In this case, kinetic terms can be ignored in the expression for the energy of a balloon configuration. For an ascent shapes, the wing sections and internal folds are the dominant fold-like features that we include in our model. Clefted material is observed while the balloon is in the spool or shortly after launch, so we will not attempt to model clefts in this work.

Observations of a model balloon at the Wallops Flight Facility suggested that it would be reasonable to model ascent shapes of balloons as asymmetric shapes generated using symmetries and a fundamental section.[4] For our model ascent shapes, we will consider shapes that are invariant under the action of the dihedral symmetry group D_k. A shape with D_7 symmetry has the symmetries of a heptagon. The construction of an asymmetric shape is discussed further in Sec. V.

In this work, we will speak of circumferential balloon fibers and meridional balloon fibers. These are easiest to identify in the float shape. For this paper, the tail of the balloon is located at the origin of our coordinate system, and the central axis of the balloon lies

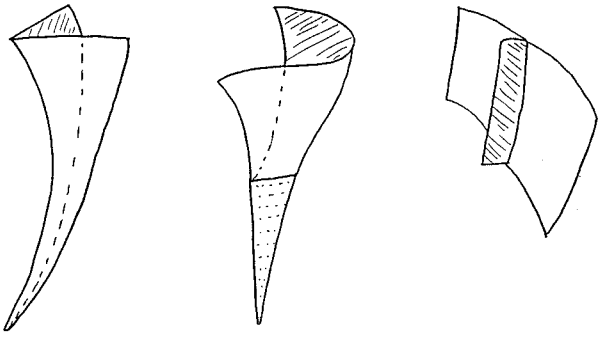

Fig. 2 Fold-like features of ascent shapes: cleft (left), wing (middle), and internal fold (right).

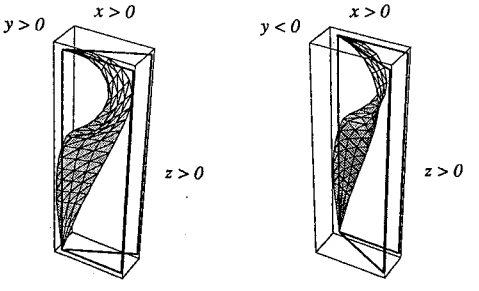

Fig. 3 $\mathcal{S}_{\text{fund}}$ (left) and $\mathcal{S}'_{\text{fund}}$ (right).

along the positive z axis. A circumferential fiber can be obtained by intersecting the float shape with a plane parallel to the $z = 0$ plane. Because the float shape is a surface of revolution, the circumferential fibers are circles (see Fig. 1). A meridional fiber can be obtained by intersecting the float shape with a plane that contains the z axis (see Fig. 1). In our model of ascent shapes, we will assume that the lengths of circumferential and meridional fibers are fixed. In an ascent shape, these fibers will deform (without stretching) from their respective positions in the float configuration.

Winker[5] identified two important planar curves which are observed in off-design (ascent) shapes. These planar curves, named the hook and wing profiles in Ref. 4, lie in two planes which define the planes of reflective symmetry in our model, namely, the hook plane $\mathcal{P}_{\text{hook}}$ and the wing plane $\mathcal{P}_{\text{wing}}$. By requiring that the off-design shape have dihedral symmetry, preserving the lengths of circumferential and meridional balloon fibers, and requiring that excess fiber material be contained within a fold running along the hook profile, we are able to construct an off-design balloon shape that has many features of an actual balloon. All our model assumptions are consistent with observations of actual balloons.

In Fig. 3, we present the fundamental section $\mathcal{S}_{\text{fund}}$ of an off-design balloon with D_7 (heptagonal) symmetry and $\mathcal{S}'_{\text{fund}}$, its reflection in the hook plane. The hook and wing profiles are based on data presented in Ref. 5. Outlines of $\mathcal{P}_{\text{hook}}$ and $\mathcal{P}_{\text{wing}}$ can be seen in Fig. 3. Figure 4 shows the components of a complete off-design shape, seven pairs of $\mathcal{S}_{\text{fund}}$ and $\mathcal{S}'_{\text{fund}}$. The shape $\mathcal{S}_{\text{fund}}$ presented in Fig. 3 is not at equilibrium but will be used as the initial guess for our method which will evolve the shape to equilibrium. Although $\mathcal{S}_{\text{fund}}$ will change, the evolved shapes will remain inside the wedge $\mathcal{W} = \{(x, y, z) \in R^3 \mid 0 \leq y \leq \tan(\pi/k)x\}$ (for viewing purposes, we display portions of internally folded material outside the set $\mathcal{W}$).

It was pointed out in Ref. 4 that material constraints defined by the float shape influence the type of asymmetric ascent shapes that are possible. Consider a circumferential fiber, say, below the gas bubble. If the hook and wing profile curves are known, the shortest distance from corresponding stations on these two curves is a straight line. One can verify that octagonal symmetry is not possible with the hook and wing profiles in Fig. 3 because there would be insufficient material to form complete loops for certain circumferential fibers.[4] Thus, there is a limit to the number of symmetries that are possible for a given pair of profile curves. Whereas the profile curves are in general not known a priori, it is clear that certain asymmetric shapes can be ruled out due to material constraints. Initially, the hook and

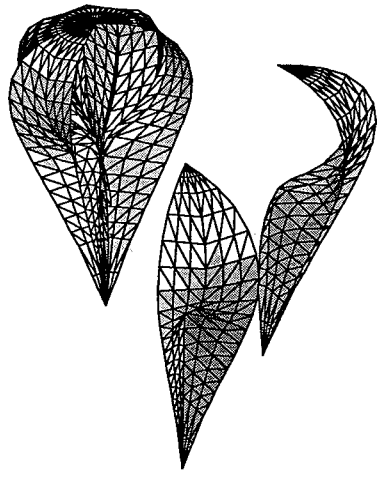

Fig. 4 Constructing a complete balloon shape with heptagonal symmetry.

wing profiles are approximated, but these curves are evolved to equilibrium along with the entire shape.

III. Variational Approach

The Σ-shape model yields axisymmetric shapes and does not generalize to nonaxisymmetric shapes. For this reason, we propose to model nonaxisymmetric shapes using a variational approach. We define the energy E of a balloon configuration as

$$E = \rho \int_{\mathcal{V}} z \, dV + \mu \int_{S} z \, dS \tag{1}$$

where the first integral is the gravitational potential energy of the lifting gas, and the second integral is the gravitational potential energy of the balloon fabric. Because the altitude is fixed, there are no kinetic terms contributing to Eq. (1), and ρ is constant. The constant $\rho < 0$ is proportional to the difference between the densities of the lifting gas and ambient air, and μ is proportional to the film density. Here, z measures the height above some reference plane, $\mathcal{V}$ is the volume defined by the gas bubble, and S is the surface defined by the balloon film. The potential in Eq. (1) has the units of mass $\times$ acceleration $\times$ distance. It is important to note that S includes fabric that bounds the gas bubble and fabric that is internally folded. In general, the boundary of $\mathcal{V}$ is not necessarily equal to S. A shape that minimizes the energy in Eq. (1), subject to certain material constraints that are related to the inextensibility of balloon fibers and volume of the gas will be called an energy-minimizing shape.

Since the focus of this work is to model ascent shapes, we will assume that the design (float) shape is known. In particular, we will assume that the generating curve

$$(R(s), Z(s)), \qquad 0 \le s \le \ell \tag{2}$$

for the surface of revolution of the float shape and its length ℓ are known. The parametrization is obtained by solving the Σ-shape equations with the appropriate boundary conditions. (When computing design shapes, one normally rescales the equations, see, Ref. 1. The rescaled arc length $\bar{s}$ in Ref. 1 corresponds to s in this work). The length of a meridional fiber will be denoted by ℓ and s is the arc length s, i.e.,

$$|R'(s)|^2 + |Z'(s)|^2 = 1 \tag{3}$$

The total length of a circumferential fiber at position s is given by $2\pi R(s)$. Since the parametrization (2) is known, so are the volume $\mathcal{V}_{\text{float}}$ and surface area $\mathcal{A}_{\text{float}}$.

Axisymmetric Shapes

We first formulate the discrete approximation of the model equations for an axisymmetric shape. The generating curve for such a shape will be denoted by $(r(s), z(s))$. For a surface of revolution Eq. (1) can be written in the form

$$E[r, z] = \pi\rho \int_0^{\ell} z(s) r^2(s) z'(s) \, ds + 2\pi\mu \int_0^{\ell} z(s) r(s) \, ds. \tag{4}$$

The volume $\mathcal{V}$ and gore length ℓ are fixed, i.e.,

$$\ell = \int_0^{\ell} (|r'(s)|^2 + |z'(s)|^2)^{\frac{1}{2}} \, ds \tag{5}$$

$$\mathcal{V} = \pi \int_0^{\ell} r^2(s) z'(s) \, ds \tag{6}$$

respectively. The minimization of $E[r, z]$ is done over the class of all piecewise continuously differential curves satisfying

$$r(0) = z(0) = r(\ell) = 0 \tag{7}$$

For a weightless balloon film $\mu = 0$, the Euler–Lagrange equations for Eqs. (4) and (5) are the Σ shape differential equations with $\mathcal{V}$ determined by the payload (see Ref. 2). To compute an EM shape, we first make a rough guess of the solution. The shape is evolved to equilibrium by solving a discrete approximation to the constrained minimization problem defined by Eqs. (4–7).

Approximating $(r(s), z(s))$ by a set of points

$$(r(s_k), z(s_k)) \approx (r_k, z_k), \qquad k = 0, 1, \ldots, n$$
$$0 = s_0 < s_1 < \cdots < s_{n-1} < s_n = \ell$$

we are lead to the following problem that can be used to compute axisymmetric EM shapes:

Minimize

$$E = \pi\rho \sum_{k=1}^{n} z_k r_k^2 \Delta z_k + 2\pi\mu \sum_{k=1}^{n} z_k r_k \left(|\Delta r_k|^2 + |\Delta z_k|^2\right)^{\frac{1}{2}} \tag{8}$$

subject to

$$\ell = \sum_{k=1}^{n} \left(|\Delta r_k|^2 + |\Delta z_k|^2\right)^{\frac{1}{2}} \tag{9}$$

$$\mathcal{V} = \pi \sum_{k=1}^{n} r_k^2 \Delta z_k \tag{10}$$

where $\Delta r_k = r_k - r_{k-1}$ and $\Delta z_k = z_k - z_{k-1}$.

For a Σ shape below float, we assume that excess balloon film is carried in a rope section that hangs from the base of the balloon, and so the surface area is not a constraint (although the total weight of the balloon is preserved). In our nonaxisymmetric model, the surface area of the balloon fabric will be incorporated as a constraint.

Nonaxisymmetric Shapes

For a nonaxisymmetric shape, we can derive discrete approximations for Eq. (1) and its associated constraints. This is done by approximating the smooth balloon surface by a faceted surface (see, e.g., Fig. 3 where the facets are triangles). We will follow the notation and conventions that are defined in Ref. 6. After applying the divergence theorem, the volume integral in Eq. (1) can be replaced with a surface integral, i.e.,

$$\int_{\mathcal{V}} z \, dV = \int_{\mathcal{V}} \text{div}(\boldsymbol{F}) \, dV = \int_{S} \boldsymbol{F} \cdot d\boldsymbol{A} = \int_{S} \tfrac{1}{2} z^2 \boldsymbol{k} \cdot d\boldsymbol{A} \tag{11}$$

where $\boldsymbol{k}$ is a unit vector parallel to the z axis, $\boldsymbol{F} = \frac{1}{2}z^2\boldsymbol{k}$, $\mathrm{d}\boldsymbol{A} = \boldsymbol{n}\,\mathrm{d}A$, $\boldsymbol{n}$ is a unit vector that is normal to the surface $\mathcal{S}$, $\mathrm{d}A$ is surface area measure on $\mathcal{S}$, and $\mathcal{S}$ is the boundary of the body $\mathcal{V}$ (see Ref. 6). Suppose that there are $N_{\mathcal{F}}$ facets that make up the balloon fabric (folded and unfolded material). Let $\mathcal{F}_i$ denote the ith facet. Let $\mathcal{A}_i$ denote the area of $\mathcal{F}_i$. Choose a base point on the z axis interior to the gas bubble, and let $\mathcal{V}_i$ denote the volume of the tetrahedron formed by connecting the base point to each vertex of the facet $\mathcal{F}_i$. If we apply Eq. (11) to a tetrahedron, we obtain contributions from each of its four facets. However, when we apply the divergence theorem to the entire body, only integrals over the facets $\mathcal{F}_i$ will contribute to the surface integral that represents the gravitational potential energy of the gas. Contributions made by interior facets of tetrahedra will cancel. We are lead to the following problem that can be used to compute nonaxisymmetric EM shapes:

Minimize

$$E = \rho \sum_{i=1}^{N_{\mathcal{F}}} \int_{\mathcal{F}_i} \tfrac{1}{2}z^2\boldsymbol{k}\cdot\mathrm{d}\boldsymbol{A} + \mu \sum_{i=1}^{N_{\mathcal{F}}} \int_{\mathcal{F}_i} z\,\mathrm{d}A \tag{12}$$

subject to

$$\mathcal{V} = \sum_{i=1}^{N_{\mathcal{F}}} \mathcal{V}_i \tag{13}$$

$$\mathcal{A}_{\text{float}} = \sum_{i=1}^{N_{\mathcal{F}}} \mathcal{A}_i \tag{14}$$

where $\mathcal{A}_{\text{float}}$ is the surface area of the float shape. Note, unlike the axisymmetric case, the total surface area of the balloon film is preserved for all ascent shapes. Because of the simple geometry, closed-form expressions for the integrals in Eq. (12) are available.[6] We will require that the length of a circumferential fiber must equal its length at float. Similarly, we require that meridional fiber lengths be preserved. Suppose that there are n_c circumferential and n_m meridional fibers in our faceted surface. Let $\{e^m_{k,j} \mid k = 1,\ldots,n^m_j\}$ denote the set of edge lengths that make up the jth meridional fiber. Let $\{e^c_{k,j} \mid k = 1,\ldots,n^c_j\}$ denote the set of edge lengths that make up the jth circumferential fiber. The fiber constraints can be expressed as follows:

$$\ell = \sum_{k=1}^{n^m_j} e^m_{k,j}, \qquad j = 1,\ldots,n_m \tag{15}$$

$$2\pi R(s_j) = \sum_{k=1}^{n^c_j} e^c_{k,j}, \qquad j = 1,\ldots,n_c \tag{16}$$

The balloon configuration is defined by specifying the positions of all the external vertices. Any excess circumferential fiber material must be contained within an internal fold that lies in $\mathcal{P}_{\text{hook}}$. The endpoints of these fibers are vertices of the faceted surface. However, the corresponding facets do not contribute to the first sum in Eq. (12), because they are not part of the boundary of the gas bubble. The internally folded material is chosen so that Eq. (16) is satisfied. Because of the symmetry of an EM shape, only the fundamental section (i.e., the one lying in $\mathcal{W}$) is solved for. In particular, if (x_j, y_j, z_j) are the vertices of the fundamental section, we require that

$$0 \le y_j \le \tan(\pi/k)x_j, \qquad j = 1,\ldots,N_v \tag{17}$$

IV. Axisymmetric Shape Computations

In this section, we will present numerical results for the constrained optimization problem defined by Eqs. (4–6). We will compute shapes for two cases. In case I, $\mathcal{V} = \mathcal{V}_{\text{float}}$ and in case II, $\mathcal{V}$ is approximately 16% of $\mathcal{V}_{\text{float}}$. The energy is a function of $(r_0, z_0), \ldots, (r_n, z_n)$, where $(r_0, z_0) = (0, 0)$, $r_n = 0$, and $n = 16$. EM shapes are found by solving Eqs. (8–10) with Matlab software constr which requires an initial guess for the solution. We assume an initial configuration of a hemisphere on a cone with gore length and volume approximately equal to ℓ and $\mathcal{V}_{\text{float}}$ respectively.

Constr generates a sequence of shapes that converges to an equilibrium configuration that minimizes the energy and satisfies all constraints. Constr implements a sequential quadratic programming method by Powell.[7] We will refer to this solution process as an evolution. Figure 5 shows a subsequence of shape profiles which were evolved in this fashion. The target gore length was $\ell = 2.870569$. The target volume was $\mathcal{V} = \mathcal{V}_{\text{float}} = 3.4383$. These values correspond to the case $\Sigma = 0.4$ (see Ref. 1 for the definition of Σ). Intermediate shapes in the solution process need not satisfy all constraints. The last shape shown in Fig. 5 agrees with the expected Σ-shape profile. In case II, the target volume was reduced to 16% of $\mathcal{V}_{\text{float}}$. Data on the initial guess and EM shape for cases I and II are presented in Table 1. The maximum radius of a shape is $r = r^*$ and occurs when $z = z^*$. In Table 2, EM-shape parameters are compared to the corresponding design values that are computed from the Σ-shape model.

Table 1 Comparison of initial and evolved shapes

	Case I $\mathcal{V} = \mathcal{V}_{\text{float}}$		Case II $\mathcal{V} = 0.16 \cdot \mathcal{V}_{\text{float}}$	
Quantity	Initial	Evolved	Initial	Evolved
E	−2.482	−3.0223	−0.985	−1.0727
E_{gas}	−2.5	−3.0440	−0.9998	−1.0875
E_{film}	0.0186	0.0217	0.0148	0.0147
$\mathcal{V}$	3.15	3.4363	0.5521	0.5628
ℓ	2.839	2.8716	2.864	2.8706
$\mathcal{A}$	11.03	11.2547	4.016	3.6273

Table 2 Comparison of EM shapes and Σ-shapes

	Case I $\mathcal{V} = \mathcal{V}_{\text{float}}$		Case II $\mathcal{V} = 0.16 \cdot \mathcal{V}_{\text{float}}$	
Quantity	Σ shape	EM shape	Σ shape	EM shape
$z_{\max}$	1.5912	1.5857	2.4011	2.421
r^*	1.036	1.031	0.517	0.507
z^*	0.937	0.976	2.048	2.035
θ_0 deg $\approx$	70.2	67.9	0.50	0.69
$\mathcal{V}$	3.4383	3.4363	0.5628	0.5628
ℓ	2.870569	2.8716	2.870569	2.8716
$\mathcal{A}$	11.2814	11.2547	3.6273	3.6296

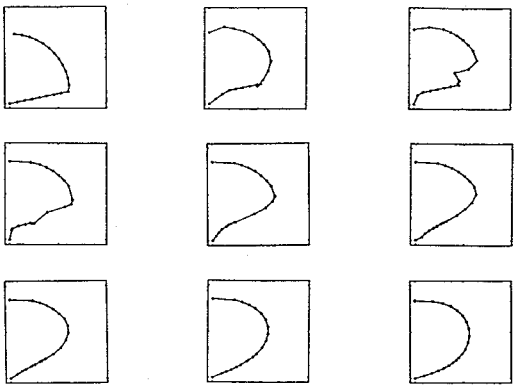

Fig. 5 Evolution of an axisymmetric EM shape at float.

The results on the EM shapes presented in Table 2 agree to within 10^{-2} when compared to the corresponding Σ-shape results, the corresponding Σ shapes for cases I and II are shown in Fig. 1. Our purpose was not to reproduce the Σ shapes here, but to determine if we could obtain reasonable agreement using our EM model. Our axisymmetric EM shapes are sufficiently close to the Σ shapes to motivate the study of nonaxisymmetric shapes with a variational approach based on the energy defined in Eq. (1).

V. Nonaxisymmetric Shape Computations

Our approach to modeling nonaxisymmetric balloon shapes is to minimize the energy E in Eq. (12) subject to constraints Eqs. (13–17). The minimization is done with respect to a class of surfaces $\mathcal{C}_k$ that are invariant under D_k and piecewise continuously differentiable. We assume that the hook and wing profiles are planar curves that lie in $\mathcal{P}_{\text{hook}}$ and $\mathcal{P}_{\text{wing}}$, respectively. Continuity of the shapes in

Table 3 EM shape with heptagonal symmetry

Quantity	Initial	Target values	Evolved
E	−1.2034	——	−1.0867
E_{gas}	−1.2357	——	−1.1208
E_{film}	0.03232	——	0.03416
$\mathcal{V}$	0.64168	0.56278	0.5638
$\mathcal{A}$	10.77388	11.2487	11.2618
Gore length,	$\ell \pm 0.054$	$= 2.870569$	± 0.028
$z_{\max}$	2.3812	——	2.3955

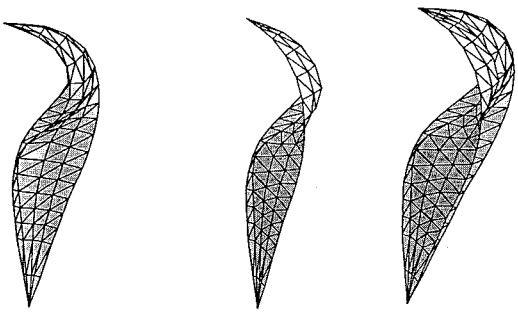

Fig. 6 $\mathcal{S}_{\text{fund}}$, $\mathcal{S}'_{\text{fund}}$ **and** $\mathcal{S}_{\text{fund}} \cup \mathcal{S}'_{\text{fund}}$ **after evolving.**

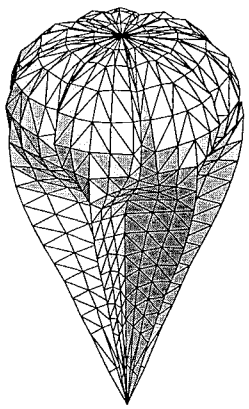

Fig. 7 Heptagonal EM shape.

$\mathcal{C}_k$ imply that the profile curves remain in these respective planes. Any excess circumferential fiber material will be folded away in a segment that lies in the hook plane.

To illustrate how the folding is modeled, we describe the construction of the shape with heptagonal symmetry that is presented in Fig. 3. The initial hook and wing profiles are obtained from Ref. 5 (also see Ref. 4). Let $\{s_k\}$ with

$$0 = s_0 < s_1 < \cdots < s_{n_m} < s_{n_m+1} = \ell$$

denote a set of points along a meridional fiber in the float shape. Identify points on the hook and wing profiles corresponding to s_k and join them with a fiber of length $1/7\pi R(s_k)$. To make a closed circumferential fiber loop of length $2\pi R(s_k)$ requires 14 segments. One end of the fiber lies on the wing profile, whereas the other end of the fiber is free to slide through the corresponding point on the hook profile. If the points on the hook and wing profiles are joined by a straight line, there may be excess fiber, which is then folded into the hook profile plane. Endpoints of the excess fibers define vertices which join to form edges of facets that represent excess folded fabric. Note, inside the gas bubble, excess material appears as an internal fold. Below the gas bubble, excess material is distributed within the flat lower wing section. The precise distribution is unknown.

As previously stated, $\mathcal{S}_{\text{fund}}$ in Fig. 3 is not at equilibrium, nor are all of the constraints satisfied. The energy and constraints can be expressed as functions of the external vertices. To obtain an EM shape, we utilized the Matlab routine constr to solve the constrained minimization problem defined by Eqs. (12–17) with $n_m = 4$ and $n_c = 17$. Figure 6 shows the fundamental section of an EM shape with heptagonal symmetry that was evolved from the initial shape presented in Fig. 3. Configurations that were evolved from $\mathcal{S}'_{\text{fund}}$ and $\mathcal{S}_{\text{fund}} \cup \mathcal{S}'_{\text{fund}}$ are presented also in Fig. 6. Figure 7 shows the entire EM shape. In Table 3, we present data corresponding to the initial and evolved shapes. The target volume was set to approximately 16% of $\mathcal{V}_{\text{float}}$. The target gore length and surface area are presented in Table 3. All target constraints were met to within 1%. Given the simplifying assumptions that were made on defining the faceted surface, we felt this level of accuracy was acceptable.

VI. Concluding Remarks

By considering the gravitational potential energy of a balloon, we are able to compute EM shapes by solving a constrained minimization problem. When we assume an axisymmetric shape in our model, we find that our EM shapes agree with the Σ shapes that are obtained by solving the standard Σ-shape model (see Sec. IV). We model nonaxisymmetric shapes by minimizing the energy over a class of asymmetric shapes $\mathcal{C}_k$ that possess dihedral symmetry D_k for some k. Shapes in $\mathcal{C}_k$ admit fold-like features that characterize ascent shapes of actual balloons. In Sec. V, we presented a heptagonal ascent shape that was computed in this fashion. Our approach could be applied to obtain shapes with other dihedral symmetries. Our model leads to energy minimizing nonaxisymmetric balloon shapes that possess internal folds of excess material inside the gas bubble and flat wing sections below the gas bubble. Other features reflected in solutions of our model include a sphere-like top and periodic lobes surrounding the gas bubble. These are features that are observed in the ascent shapes of real balloons. Our variational approach for computing EM shapes was the first successful attempt at modeling nonaxisymmetric ascent shapes that captured significant geometric features of actual balloon shapes.

Acknowledgment

The authors were supported by NASA Grant NAG5-697. Work was initiated by the principal author under a 1992 NASA/ASEE Summer Faculty Fellowship at NASA/GSFC/WFF Balloon Projects, Wallops Island, Virginia. The authors would also like to thank Willi Schur for suggesting the variational approach for computing balloon shapes. The authors are grateful to the reviewers for a number of comments that helped clarify several important points.

References

[1]Morris, A. L. (ed.), "Scientific Ballooning Handbook," NCAR Tech. Note, NCAR TN-99, National Center for Atmospheric Research, Boulder, CO, 1975, Sec. V, pp. 1–45.

[2]Anon., "Research Development in the Field of High Altitude Plastic Balloons," Univ. of Minnesota, Dept. of Physics, Minneapolis, MN, 1951–1956, NONR-710(01) Reports, pp. 3–12.

[3]Smalley J. H. "Balloon Shapes and Stresses Below the Design Altitude," National Center for Atmospheric Research, NCAR-TN-25, Dec. 1966.

[4]Baginski, F., "Mathematical Modeling of Off-Design Balloon Shapes," 1992 NASA/ASEE Summer Faculty Fellowship Program Final Rept., submitted to the NASA/GSFC/WFF Balloon Projects Branch, Aug. 1992.

[5]Winker, J. A., "Stress Patterns, Shape Studies and Failure Analysis on Real Balloons," AIAA Paper 86–2518, 1986.

[6]Brakke, K., *The Surface Evolver Manual*, Version 1.91, Geometry Center, Minneapolis, MN, May 1993.

[7]Powell, M. J. D., "A Fast Algorithm for Nonlinearly Constrained Optimization Calculations," *Numerical Analysis*, edited by G. A. Watson, Lecture Notes in Mathematics, Springer–Verlag, New York, Vol. 630, 1978.